On the electrophoretic mobility of isolated colloidal spheres

2004 J. Phys.: Condens. Matter 16 3835

(http://iopscience.iop.org/0953-8984/16/23/004)

INSTITUTE OF PHYSICS PUBLISHING JOURNAL OF PHYSICS: CONDENSED MATTER

J. Phys.: Condens. Matter **16** (2004) 3835–3842 PII: S0953-8984(04)75827-0

On the electrophoretic mobility of isolated colloidal spheres

Norbert Garbow[1], **Martin Evers**[1], **Thomas Palberg**[1] **and Tsuneo Okubo**[2]

[1] Universität Mainz, Institut für Physik, Staudinger Weg 7, D-55128 Mainz, Germany
[2] Department of Applied Chemistry, Gifu University, Gifu 501-1193, Japan

Received 5 February 2004
Published 28 May 2004
Online at stacks.iop.org/JPhysCM/16/3835
DOI: 10.1088/0953-8984/16/23/004

Abstract

We studied the electrophoretic mobility μ of highly charged colloidal spheres in very dilute low salt aqueous suspension. We combined experiments on individual particles and ensemble averaged measurements. In both cases μ was observed to be independent of particle size and surface chemistry. Corresponding effective charges Z^*_μ, however, scaled with the ratio of particle size to Bjerrum length λ_B: $Z^*_\mu = Aa/\lambda_B$ with a coefficient $A \approx 2$. Our results are discussed in comparison to other charge determination experiments and charge renormalization theory and with respect to the issue of charge polydispersity.

(Some figures in this article are in colour only in the electronic version)

1. Introduction

By definition, colloidal suspensions consist of particles in the size range between 10 nm and 10 μm immersed in a solvent. Their properties are of vital interest in a vast range of applications ranging from nanotechnology to biology. In particular, charged systems have attracted considerable interest. Important aspects comprise their stability against aggregation (usually discussed in terms of the celebrated DLVO theory [1]), their ability to form ordered structures [2, 3], and their transport properties within and without external fields [1, 4, 5]. For charged particles the interaction with electric fields is of particular interest. Subjected to a homogeneous electric field of strength E, charged spheres will acquire a constant drift velocity $v = \mu E$, where μ is their electrophoretic mobility. Knowledge of this transport coefficient has two important applications: first, it will contribute to describing and understanding a number of interesting phenomena occurring upon manipulation of colloidal spheres with electric fields, e.g. pattern formation in electrodeposition [6] or annealing of crystallite defects in drying colloidal films [7]. Second, it may serve as a measure of particle charge and thus to determine particle stability and interactions: the charge is connected to the electrokinetic surface or ζ-potential which in turn determines the mobility. Mean field and more sophisticated theoretical treatments of the former relation are available for both non-interacting and strongly interacting

(even crystalline ordered) particles [1, 8–11], while the latter connection is more difficult and at present only single particle theories are available [12–14].

Measurements of the mobility have been performed mainly in the salt rich limit, which corresponds to situations where stability is an issue and to biological environs. Here we are interested in the mobility under near salt free conditions, which are typical for the formation of charged colloidal crystals. Measurements of this kind are generally rare but have been pursued in our group for some time [15–21]. Of special interest for the present study is the recently reported observation of a logarithmic particle concentration dependence of μ [18]. Given this and the theoretical situation, quantitative experiments necessitate the performance of measurements on very dilute systems or even isolated particles. Laser Doppler velocimetry (LDV) is one convenient and flexible means to determine the average mobility. It is applied here to measure μ of low salt to deionized aqueous suspensions at very low packing fractions of $\Phi = 10^{-6}$ over a large range of particle radii 45 nm $< a <$ 1500 nm. In addition we use a newly developed optical tweezing electrophoresis (OTE [19]) measuring both the size and mobility of isolated trapped spheres. For particle radii 300 nm $< a <$ 500 nm this technique enables us to check the size/mobility relation on the level of individual spheres and yields the mean mobility but also higher moments of the distribution. Here we measure the salt concentration dependence at $\Phi = 10^{-7}$ in a different solvent, a 35% (V/V) mixture of water and glycerol.

For both cases we find the mobility to first increase with decreasing salt concentration c but then to reach a plateau value for $c < 5\times10^{-5}$ mol l^{-1}. Somewhat counterintuitively the limiting values in the deionized state coincide at values of $\mu \approx (0.75 \pm 0.5)$ (μm s^{-1}) (V cm^{-1})$^{-1}$ for the water/glycerol mixture and $\mu \approx (3.5 \pm 0.5)$ (μm s^{-1}) (V cm^{-1})$^{-1}$ for the water samples. In a given solvent the mobility is thus independent of size. We first give a short outline of our experimental set-ups and describe the samples used. We then present our results and we close with a detailed discussion of some implications of our findings including the relation of the electrokinetic charge and renormalized charge [11] and of size and charge polydispersity.

2. Experimental details

Particle data are compiled in table 1. Water based samples were purified using an ultrafiltration cell followed by treatment with mixed bed ion exchange resin (AG501-X8, Bio-Rad, D) for more than ten days and dilution with Milli-Q water. For OTE, samples were conditioned in a closed tubing system using mixed bed ion exchange resin (Amberlite UP 604, Rohm & Haas, F) [22]. For the deionized systems, the residual salt concentration is given by the dissociation product of water to be 10^{-7} mol l^{-1}, in good agreement with measured conductivities. Salt concentrations were adjusted under inert gas atmosphere to avoid contamination with airborne CO_2. All measurements were performed at 25 °C. Water samples were investigated using a commercial laser Doppler velocimetric set-up (Laser Zee Meter 501, Pen Kem Inc., Bedford Hills, NY).

Water/glycerol samples were investigated by OTE using a straightforward modification of the single particle tracking apparatus developed by Schätzel and the present authors [23]. A laser beam ($\lambda = 532$ nm) is focused through a microscope objective into the quartz optical cell containing the very dilute dispersion. Light pressure pushes individual trapped particles along this optical trap. A feedback loop moving the objective in the same z-direction keeps the particle in focus. Experiments were carried out in a 35% (w/w) glycerol in water solution. The increase in η leads to tracking times of some 20 s and in addition facilitates a comparison to pure water results to check for an influence of ε_r. The back scattered light is collected on a photodetector. A combined analysis of back scattered intensity and drift velocity allows for a

Table 1. Particle data and results. Data are assorted by different solvents corresponding to different Bjerrum lengths $\lambda_B = e^2/4\pi\varepsilon_0\varepsilon_r k_B T$ (the distance over which the pair interaction energy between point-like monovalent ions equals the thermal energy), and further by increasing particle diameter $d = 2a$ (DLS: dynamic light scattering; OT: optical tweezing). We show titrated charge numbers N absolute mobilities in the deionized state as well as effective electrophoretic charges Z^*_μ evaluated using the SEM and renormalized charges calculated using a program kindly provided by Belloni [24].

Sample	λ_B (nm)	$2a$ (nm)	N	μ (2×10^{-7} M) (10^8 m^2 V^{-1} s^{-1})	Z^*_μ	Z^*_{PBC}
D1C27[b]	0.72	91 ± 6 (DLS)[a]	4.6×10^3 [a]	4.0	190	680
D1B22[b]	0.72	109 ± 3 (DLS)[a]	8.5×10^3 [a]	3.3	187	785
D1B72[b]	0.72	173 ± 7 (DLS)[a]	6.0×10^3 [a]	3.5	315	1.09×10^3
N200[c]	0.72	220 ± 5 (DLS)[a]	4.0×10^4 [a]	3.1	355	1.38×10^3
D1B33[b]	0.72	269 ± 3 (DLS)[a]	4.1×10^4 [a]	2.6	364	1.68×10^3
No. 103[e]	0.72	363 ± 30 (DLS)	7.8×10^7 [a]	5.1	965	2.51×10^3
G5301[f]	0.72	369 ± 10 (DLS)[a]	1.9×10^5 [a]	3.3	634	2.57×10^3
D1A92[b]	0.72	497 ± 6 (DLS)[a]	1.3×10^5 [a]	3.2	829	5.9×10^3
N601[c]	0.72	600 ± 12 (DLS)[a]	1.4×10^6 [a]	2.9	907	1.1×10^4
N1000[c]	0.72	1020 ± 20 (DLS)[a]	5.3×10^5 [a]	3.4	1807	—
H1001[g]	0.72	1022 ± 5 (DLS)[a]	3.5×10^7 [a]	2.8	1491	—
D1A12[b]	0.72	2020 ± 14 (DLS)[a]	5.0×10^6 [a]	3.0	3157	—
D1A35[b]	0.72	2950 ± 130 (DLS)[a]	2.4×10^7 [a]	2.9	4457	—
PS306[h]	0.92	301 ± 1.4 (OT)	1.67×10^5 [a]	0.72 ± 0.05	356	1.66×10^3
PS301[d]	0.92	322 ± 2.4 (OT)	$(2.3 \pm 0.2) \times 10^4$	0.72 ± 0.06	333	1.90×10^3
PS378[d]	0.92	375 ± 6.8 (OT)	1.13×10^5 [a]	0.79 ± 0.05	458	2.42×10^3
PS401[h]	0.92	401 ± 4.5 (OT)	2.8×10^5 [a]	0.68 ± 0.06	420	2.82×10^3
PS415[i]	0.92	438 ± 5.0 (OT)	1.48×10^5 [a]	0.63 ± 0.06	422	3.45×10^3
PS403[i]	0.92	454 ± 0.9 (OT)	1.54×10^5 [a]	0.76 ± 0.04	533	3.8×10^3

[a] As given by the manufacturer.
[b] Particle: polystyrene; surface groups: sulfate; Dow Chemical Co.
[c] Polystyrene; sulfate; Sekisui Chemicals Co.
[d] Polystyrene; sulfate; IDC.
[e] Crosslinked polystyrene, sulfonated by sulfurtrioxide; Fujii Photo Film Co.
[f] Styrene/styrenesulfate copolymer, Japan Synthetic Rubber Co.
[g] Polystyrene; carboxylated; Japan Synthetic Rubber Co.
[h] Polystyrene; carboxylated; IDC.
[i] Polystyrene; sulfate/carboxylate 50:50; IDC.

precise and calibrated determination of the trapped particle diameter [23]. For electrophoresis, sinusoidal electric fields were applied perpendicular to the optical axis. The strength E and frequency ω were chosen such as to yield small elongations $X \approx 0.1a$, while the $k_B T$-width of the trap is about $4a$. X was obtained with a resolution of a few nanometres from particle images projected onto a quadrant diode. For $E = 0$ and long times ($t > 0.1$ s), the numerically calculated mean squared displacement becomes a constant. For $E > 0$, a small periodic component of amplitude $X = \mu E/\omega$ is superimposed, from which the mobility of the trapped particle is inferred [19].

3. Results

OTE experiments were performed on the mixture of all PS species at $\Phi = 10^{-7}$ and different salt concentrations. An example is given in figures 1(a)–(c). A total of approximately 2500 particles was measured, of which 1543 were tracked for sufficiently long times to yield reliable size and mobility data. The raw data set (figure 1(b)) is thus a scatter plot of mobility versus

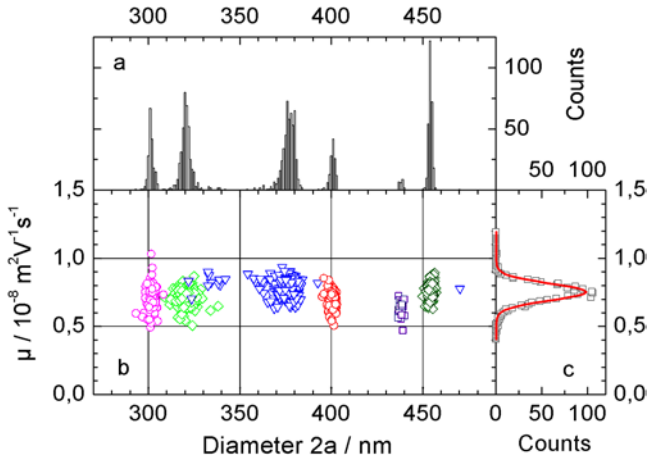

Figure 1. Scatter plot of OTE mobility and size data of individual particles in a six component mixture at $\Phi = 10^{-7}$ and $c = 10^{-5}$. Top: histogram of the size distribution. Right: histogram of the mobility distribution; the solid line is a fit of a Gaussian yielding $\mu = (0.75 \pm 0.07)10^{-8}$ m^2 V^{-1} s^{-1}.

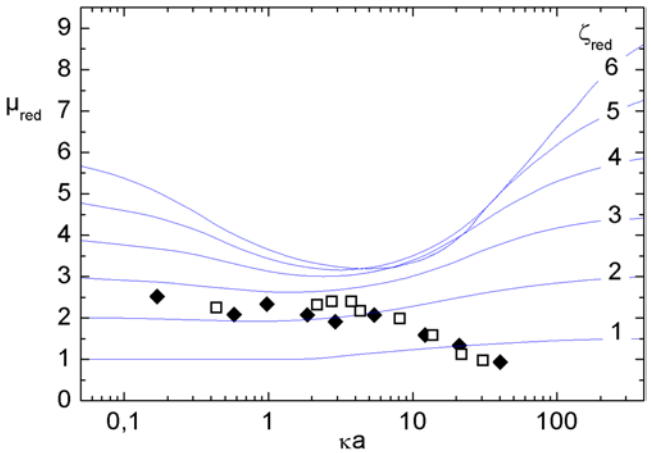

Figure 2. Reduced mobilities versus κa for the salt concentration dependent measurements on N601 in water measured with LDV (□) and PS301 in water/glycerol measured with OTE (⧫). Also shown are theoretical expectations of the standard electrokinetic model [12] (solid curves with the corresponding reduced ζ-potentials $\zeta_{\mathrm{red}} = \zeta e/k_{\mathrm{B}}T$ indicated on the right).

diameter with one point for each particle. The size distribution is given in figure 1(a) and the mobility distribution in figure 1(c). Note that all species are well resolved with respect to d; for some species even the skewness is clearly detected. The mobility distribution, however, is well fitted by a single Gaussian: $\mu_{\mathrm{avr}} = (0.75 \pm 0.07)$.

In figure 2 the reduced mobility at different salt concentrations is plotted for N601 and PS301 versus κa. Here $\kappa^2 = e^2 2000 N_{\mathrm{A}} c/\varepsilon_0 \varepsilon_{\mathrm{r}} k_{\mathrm{B}} T$ defines the screening parameter with the elementary charge e, Avogadro's number N_{A}, the dielectric permittivity of the solvent $\varepsilon_0\varepsilon_{\mathrm{r}}$ ($\varepsilon_{\mathrm{r}} = 79.8$ for water and 66.9 for the mixture) and the thermal energy $k_{\mathrm{B}}T$. The reduced mobility corrects for the influence of different solvents: $\mu_{\mathrm{red}} = (2/3)\eta\mu/\varepsilon_0\varepsilon_{\mathrm{r}}k_{\mathrm{B}}T$ with solvent viscosity η (0.965 cP for water and 2.6 cP for the mixture). Note that the lowest attainable κa differs for the two species due to both different radii and solvents.

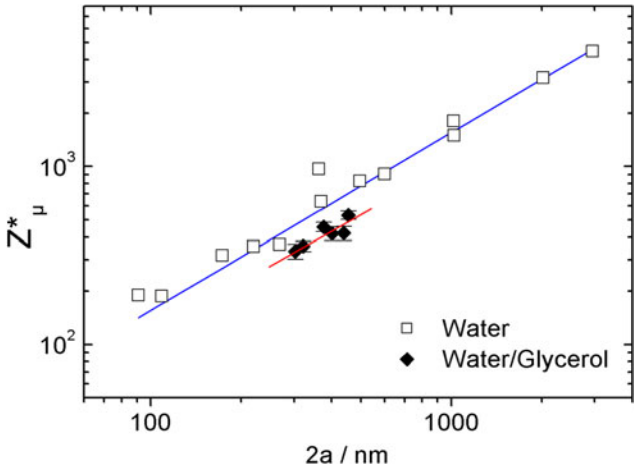

Figure 3. Effective electrophoretic charge versus particle diameter: double logarithmic plot. Charges were calculated from the limiting values of μ for $c = 2 \times 10^{-7}$ mol l^{-1} using SEM [12] and a Debye–Hückel effective potential. Open symbols: water samples at $\Phi = 10^{-6}$, LDV; closed symbols: water/glycerol samples, OTE. The lines are fits through the origin and the data of $Z^*_\mu = Aa/\lambda_B$ yielding $A = 2.24 \pm 0.07$ for the water samples and $A = 2.04 \pm 0.06$ for the mixed solvent samples.

With decreasing c, μ_{red} first increases but is approximately constant for $c < 5 \times 10^{-5}$ mol l^{-1}. This applies for both species which are of comparable size and surface chemistry but show more than an order of magnitude difference in N. In fact, very similar behaviour was also observed for the other samples. We performed fits of straight lines through the values for $c < 5 \times 10^{-5}$ mol l^{-1}. The fit values of μ for complete deionization are compiled in table 1. With the exception of No. 103, they are of the order of 3.5×10^{-8} m^2 V^{-1} s^{-1} for the water sample, while for the mixed solvent we find them to be of the order of 0.76×10^{-8} m^2 V^{-1} s^{-1}. The main result of our study is thus that *isolated* particles of vastly different sizes, surface chemistry and titrated charge numbers show the same reduced mobilities at low salt conditions.

To evaluate mobilities for ζ-potentials and further for particle charges, several procedures are available on different levels of sophistication [1, 12–14]. Here we use the so-called standard electrokinetic model (SEM) which accounts for electrostatics, retardation (small ion currents) and relaxation effects (double layer polarization). SEM does not account for the so-called anomalous surface conduction which is accounted for in the dynamic Stern layer model of Zukoski and Saville [13]. ζ is then equated to a surface potential of Debye–Hückel type $\zeta \equiv \Psi_{DH} = Z^*_\mu e/4\pi\varepsilon_0\varepsilon_r a(1+\kappa a)$ which is solved for Z^*_μ to obtain the effective electrophoretic charges compiled in table 1.

4. Discussion

Two observations are immediately apparent from an inspection of the different charge numbers of table 1: (a) $Z^*_\mu \ll N$, and (b) there is no clear correlation between Z^*_μ and N, rather Z^*_μ seems to be proportional to a. This is also seen from figure 3, where the data are plotted in a double logarithmic fashion and are observed to arrange on straight lines. The first finding may have two reasons. In general, electrophoresis is believed to measure the dissociated charge Z, which due to incomplete dissociation will be smaller than N. However, an evaluation for effective degrees of dissociation starting from Z^*_μ yields effective surface pKs of 4–9 not compatible with the manufacturers' information on the nature of surface groups [15, 19]. In addition, we performed

calculations of the dissociated charge Z_{PBC} using a program kindly provided by Belloni [24]. It numerically solves the non-linearized Poisson–Boltzmann equation within a spherical Wigner–Seitz cell under conditions of constant surface pK. We found that $Z_\mu^* \ll Z_{\mathrm{PBC}} < N$, but even for weak acid groups (pK $= 4.5$ for carboxylate groups) the reduction did not exceed two orders of magnitude. For strong acid groups $Z_\mu^* \ll Z \tilde{=} N$. Also there is no clear correlation between Z and N.

Low Z_μ^* values may also originate from neglecting the anomalous surface conduction which leads to smaller μ values than expected by SEM. Unfortunately, we do not have a numerical implementation of the dynamic Stern layer model available and thus cannot check this presumption.

Concerning the second point, we checked possible correlations of Z_μ^* with N, Z, surface charge density, surface pK, radius a and solvent dielectric constant. Only for the latter two cases was a clear correlation observed. This is shown in figure 3, where we plot our results in a double logarithmic fashion versus particle size. With the exception of No. 103, the data arrange on a straight line of slope one over more than an order of magnitude for the water sample. Also the mixed solvent data are compatible with a linear dependence on a. The absolute values of Z_μ^* are larger for the mixed solvent sample due to the larger ε.

This kind of scaling has been observed before for other effective charges, and in fact is theoretically expected in the framework of charge renormalization, a concept originally introduced by Alexander *et al* [8]. Within a spherical Wigner–Seitz cell, the authors first obtained a numerical solution of the Poisson–Boltzmann equation and then fitted a Debye–Hückel potential at the cell boundary to obtain an effective charge Z_{PBC}^* and an effective screening parameter κ^* to the obtained solution. The most important finding was a saturation of Z_{PBC}^* with increasing Z and a scaling of the saturation value as $Z_{\mathrm{PBC}}^* = Aa/\lambda_{\mathrm{B}}$, where A is a factor of order 10. Since, the renormalization concept has been supported by further theoretical work and a number of detailed experimental studies [25–30]. Interestingly, under deionized conditions the surface potential also shows saturation with decreasing c [18, 19] and increasing Z [31]. The physical interpretation of this effect is a condensation of counterions in the vicinity of the particle surface modified by the presence of the double layers of neighbouring particles. Charge renormalization has found numerous application from soft matter physics to biology [32, 33] despite the fact that there remain subtle quantitative differences between different theoretical implementations and experimental techniques [30, 32]. Only recently it was suggested to apply the effective charge concept also to electrophoresis [34, 35]. Following this line we find $Z_\mu^* = Aa/\lambda_{\mathrm{B}}$ with $A = 2.24 \pm 0.07$ for the water samples and $A = 2.04 \pm 0.06$ for the mixed solvent samples. The slight 10% difference in A may originate from an initial particle concentration dependence. Starting from isolated particles, μ has been observed to increase logarithmically for increased Φ. Nevertheless both A nearly coincide. The deviation of A from theoretical expectations ($A \approx 10$) is possibly due to a systematic underestimation of ζ within SED. Therefore Z_μ^* qualitatively shows the scaling predicted by renormalization concepts.

We finally compare our results to those obtained by different methods in figure 4. The largest A are obtained from conductivity; those from elasticity measurements are slightly lower [30]. For both, there is a slight decrease of A with N. For electrophoresis the data for both sample series practically coincide. The decrease is even less pronounced and A values are much smaller. The differences in A have been attributed to the measurement of different properties in the respective experiments [30]. Conductivity measures the number of freely moving counterions, while elasticity is sensitive to the first and second derivative of the pair potential. Electrophoresis, on the other hand, measures the surface potential itself. Qualitatively we therefore are tempted to attribute the observed differences in A to experiment-specific

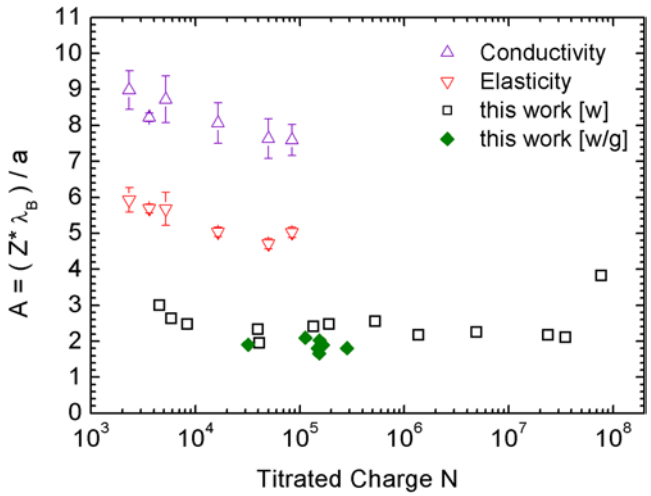

Figure 4. Comparison of the N dependence of A for different experiments. Up triangles: Z^* obtained from conductivity [29, 30]; down triangles Z^* obtained from elasticity [30]; open squares: LDV, water samples; filled diamonds: OTE water/glycerol samples. All data show a slight decrease of A with N, which is least pronounced for the present data. The latter practically coincide for both measurement series.

realizations of the same underlying effect. We note further that the quantitative differences may possibly become much smaller using an evaluation employing the dynamic Stern layer model. It thus appears that electrophoresis indeed measures *renormalized* surface potentials, and charges. We note, however, that the present study was conducted on isolated spheres, while the other experiments studied colloidal fluids and crystals. Our observation should therefore be carefully tested by future experiments on strongly interacting samples.

5. Conclusion

In conclusion, we have performed measurements of the mobility for a large number of isolated colloidal spheres under low salt conditions. For a given solvent, we find the mobility to be independent of particle size. For the manipulation of colloids this is good (relaxing) news, as size will not matter for the motion of individual colloidal spheres in external electric fields. We further showed that effective electrophoretic charges obey the scaling relation proposed for renormalized charges. Our findings thus support the proposal that electrophoresis measures renormalized charges. We finally address an immediate consequence of that result. Colloids are synthesized with narrow but unavoidably finite size distributions. This creates a major obstacle to theoretical predictions of colloid properties, because up to now it is not clear how a size polydispersity relates to a charge polydispersity and thus pair interaction polydispersity. Gisler *et al* [36] reported measurements of the static structure factor in suspensions of highly charged spheres which were compatible with the ad hoc assumption of $Z^* \propto a^2$, i.e. a scaling with the particle surface area. Phalkornkul *et al* [37] conducted similar experiments on less charged silica spheres and found reasonable agreement approximating Z^* as constant. In both cases the data were explicable with the assumed models. However, static properties in general are not very sensitive to the choice of interaction details. Fits of the structure factor in particular require additional information or assumptions (e.g. the choice of a suitable closure relation within an Ornstein–Zernicke approach [38]). Given the restricted range of particle sizes investigated in [36, 37], it is therefore not surprising that seemingly conflicting results

may occur. In the present paper we have shown on the level of individual particles that μ is independent of a (cf figure 1). We thus propose that, given the bare charge is above the saturation threshold for Z^*, a size polydispersity directly translates to an effective charge polydispersity as predicted by charge renormalization. This may have immediate impact for the calculation of colloidal suspension properties within statistical mechanics.

Acknowledgments

It is a pleasure to thank H Ohshima, H H v Grünberg, Y Levin, E Trizac and L Belloni for interesting discussions and L Belloni also for the PBC program. Financial support of the Material Research Centre (MWFZ), Mainz and the DFG (SFB 625, TPB3; SFB TR6, TPB1 and Pa 459/11) are gratefully acknowledged.

References

[1] Lyklema J 1993–2000 *Fundamentals of Interface and Colloid Science* vol 1–3 (London: Academic)
[2] Sood A K 1991 *Solid State Phys.* **45** 1
[3] Banchio A J, Nägele G and Bergenholtz J 2000 *J. Chem. Phys.* **113** 3381
[4] Nägele G 1996 *Phys. Rep.* **272** 217
[5] Banchio J, Nägele G and Bergenholtz J 1999 *J. Chem. Phys.* **111** 8721
[6] Ristenpart W D, Aksay I A and Saville D A 2003 *Phys. Rev. Lett.* **90** 128303
[7] Schöpe H J 2003 *J. Phys.: Condens. Matter* **15** L533–40
[8] Alexander S *et al* 1984 *J. Chem. Phys.* **80** 5776
[9] Groot R D 1991 *J. Chem. Phys.* **94** 5083
[10] Bocquet L, Trizac E and Aubouy M 2003 *J. Chem. Phys.* **117** 8138
[11] Levin Y 2002 *Rep. Prog. Phys.* **65** 1577
[12] O'Brien R W and White L R 1978 *J. Chem. Soc. Faraday Trans.* II **74** 1607
[13] Zukoski C F and Saville D A 1986 *J. Colloid Interface Sci.* **114** 32
Zukoski C F and Saville D A 1986 *J. Colloid Interface Sci.* **114** 45
[14] Ohshima H 2003 *Colloids Surf.* A **222** 207
[15] Okubo T 1987 *Ber. Bunsenges. Phys. Chem.* **91** 1064
[16] Deggelmann M, Palberg T, Hagenbüchle M, Maier E E, Krause R, Graf C and Weber R 1991 *J. Colloid Interface Sci.* **143** 318–26
[17] Deggelmann M, Graf C, Hagenbüchle M, Hoss U, Johner C, Kramer H G, Martin C and Weber R 1994 *J. Phys. Chem.* **98** 364
[18] Evers M, Garbow N, Hessinger D and Palberg T 1998 *Phys. Rev.* E **57** 6774–84
[19] Garbow N, Evers M and Palberg T 2001 *Colloids Surf.* A **195** 227–41
[20] Medebach M and Palberg T 2003 *J. Chem. Phys.* **119** 3360–70
[21] Medebach M and Palberg T 2003 *Colloids Surf.* A **222** 175–83
[22] Wette P, Schöpe H-J, Biehl R and Palberg T 2001 *J. Chem. Phys.* **114** 7556–62
[23] Garbow N *et al* 1997 *Physica* A **235** 291
[24] Belloni L 1998 *Colloids Surf.* A **140** 227–43
[25] Groot R D 1991 *J. Chem. Phys.* **94** 5083
[26] Bocquet L, Trizac E and Aubouy M 2003 *J. Chem. Phys.* **117** 8138
[27] Bucci S, Fagotti C, Degiorgio V and Piazza R 1991 *Langmuir* **7** 824
[28] Quesada Pérez M, Callejas Fernández J and Hidalgo Álvarez R 2001 *J. Colloid Interface Sci.* **233** 280–5
[29] Hessinger D, Evers M and Palberg T 2000 *Phys. Rev.* E **61** 5493–506
[30] Wette P, Schöpe H J and Palberg T 2002 *J. Chem. Phys.* **116** 10981–8
[31] Ohshima H 2002 *J. Colloid Interface Sci.* **247** 18
[32] Belloni L 2000 *J. Phys.: Condens. Matter* **12** R549
[33] Levin Y 2002 *Rep. Prog. Phys.* **65** 1577
[34] Fernandez-Nieves, Fernandez-Barbero A and de Las Nieves F J 2000 *Langmuir* **16** 4090
Quesada Pérez M, Callejas Fernández J and Hidalgo Álvarez R 2001 *J. Coll. Interface Sci.* **233** 280
[35] Ohshima H 2003 *Colloids Surf.* A **222** 207
[36] Gisler T *et al* 1994 *J. Chem. Phys.* **101** 9924
[37] Phalkornkul J K *et al* 1996 *Phys. Rev.* E **54** 661
[38] Krause R, Dáguanno B, Mendez-Alcaraz J M, Nägele G, Klein R and Weber R 1991 *J. Physique Coll.* **3** C3 4459